

# Semi- active vibration control of a double shell railway car-body model using bonded Piezo-electric Patch Configuration and an integrated shunt circuit

\*Silabhadra Das<sup>1</sup>, Ashish Gupta<sup>1</sup>, Yukinori Kobayashi<sup>2</sup>, Katsuya Yamamoto<sup>3</sup>, Tadao Takigami<sup>3</sup>, Mineyuki Asahina<sup>3</sup>, Takanori Emaru<sup>2</sup>, Ankit Ravankar<sup>2</sup>

<sup>1</sup> Graduate School of Engineering Hokkaido University, Sapporo

<sup>2</sup> Faculty of Engineering Hokkaido University, Sapporo

<sup>3</sup> Railway Technical Research Institute, Tokyo

**Abstract** Lighter Railway car-bodies are preferred for High Speed Rail Transport due to its fuel efficiency. Vertical bending vibrations in low frequency range of 0-10 Hz become prominent in light car-bodies. This study aims to suppress low frequency bending vibrations of a 1/12<sup>th</sup> scale car-body model by connecting a tuned multi-mode shunt circuit across the terminals of a Piezo-electric Patch Configuration (PPC) bonded to the floor of a double shell car-body. Coupled field analysis is simulated in ANSYS workbench and validated experimentally. The impact of varying the number of piezo-electric elements and its thickness, on damping performance, is further studied.

**Key Words:** Semi active control, Piezo-electric patch configuration, Railway car-body

## 1 Introduction

Vibration control in a railway coach or car-body is a big challenge which railway engineers are facing off late. Vibration in trains causes discomfort and fatigue to the passengers seated in the train car-body. The primary reason for vibration in railway trains is the railway wheel to rail interaction and the rail track irregularities. These give rise to lateral and vertical vibrations. Railway Bogies act as a connection between the axle and wheel set and the car-body. They may contain primary and secondary suspensions, vertical, lateral and yaw dampers etc. The suspensions and dampers are designed to damp the lateral and vertical vibrations originating from the wheelsets. These bogie suspensions and dampers effectively damp high frequency vibrations but are ineffective in damping low frequency vibrations [1].

In order to achieve higher speeds and improved specific fuel consumption, railway production units are manufacturing lighter railway car-bodies. Lighter car-body structures have prominent low frequency bending vibration modes. These low frequency bending vibrations are transmitted to the car-body further causing structural noise. Studies in the field of ride comfort for passengers in railway applications mention that the human body is most sensitive to vertical vibrations in the frequency range of 4-10 Hz [2]. Study conducted by Hardy et al [3] shows that structure borne noise transmission are dominant at low frequencies.

It is evident from above that low frequency bending

vibration needs to be suppressed in the railway car-body structure itself. There have been quite a few studies in the field of car-body vibration suppression in the past few years. Carlbom [4] stated that the car-body flexural modes have a significant contribution towards vertical vibrations. Takigami et al [5] used piezo-electric elements (PZT) bonded to the floor of a 1/5<sup>th</sup> scale railway car-body model and conducted passive vibration control. They further conducted vibration suppression experiments on real size car-body using Piezo-electric damping units and negative capacitance shunt circuits. Ishiguri et al [6] used a simply supported non cylindrical shell to analyze vibration characteristics of a car-body using transfer matrix method. Gautam et al [7] compared the vibro-acoustic performance of the single shell car-body model with that of the double shell model.

In this study, the problem of car-body vibration suppression will be addressed in two steps. Firstly, a suitable railway car-body model is proposed to be utilized as the objective structure. This will be done by comparing dynamic characteristics of two different car-body models namely the single shell model and the double shell model. Secondly, a semi-active vibration control methodology employing a Piezo-electric Patch Configuration (PPC) and a multi-mode shunt circuit is proposed to suppress the low frequency vibrations around the railway car-body bottom floor center. Finite Element method will be used for modelling, modal and harmonic analysis of the car-body structure in ANSYS 17.1 environment. Coupled Field Analysis is done to simulate the PPC

and the shunt circuit integrated with the car-body model. Experiments were carried out on the 1/12<sup>th</sup> scale railway car-body model to validate the simulation results.

## 2 Car-body Model

### 2.1 Single Shell Car-body Model

Preliminary analysis of vibration suppression was carried on a simplified single shell car-body model, as shown in “Fig. 1”. This model consists of a roof unit and a floor plate unit connected by aluminum conjoining joints. Physical and material specifications of this model is listed in “Table 1”.

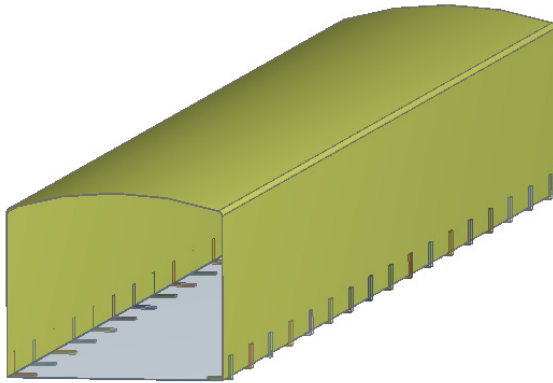


Fig .1: Single shell car-body model

**Table 1. Single shell model specification**

Car-body scaled model dimensions			Material
Sub-assembly	Parameter	Dimension (in mm)	Material
Inner shell body	Width	194.5	Stainless steel
	Height	165.5	
	Length	1670	
	Roof radius	315	
	Thickness	0.8	
Inner shell floor plate	Width	194.5	Stainless steel
	Length	1670	
	Thickness	0.8	
Conjoining clamps	Length	10	Aluminum
	Width	20	
	Height	20	
	Thickness	2	

### 2.2 Double shell Car-body Model

Double shell model consists of an inner shell hanging within an outer shell by an intermediate clamping mechanism, as in “Fig. 2”. The specifications are listed in “Table 2”.

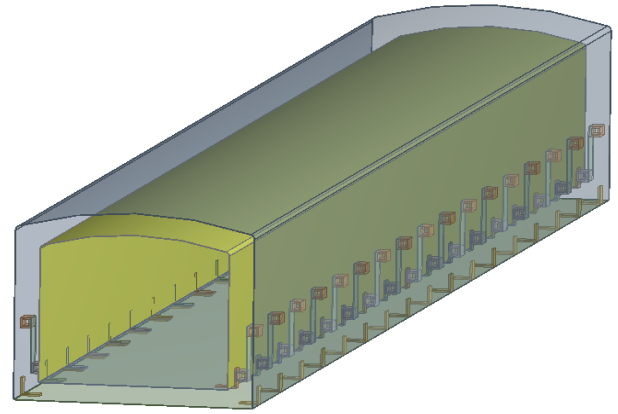


Fig .2: Double shell Car-body model

**Table 2. Double shell model Specification**

Car-body scaled model dimensions			Material
Sub-assembly	Parameter	Dimension (in mm)	Material
Inner shell body	Width	194.5	Stainless steel
	Height	165.5	
	Length	1670	
	Roof radius	315	
	Thickness	0.8	
Inner shell floor plate	Width	194.5	Stainless steel
	Length	1670	
	Thickness	0.8	
Conjoining clamps	Length	10	Aluminum
	Width	20	
	Height	20	
	Thickness	2	
Intermediate clamps	Height	61	Aluminum
	Thickness	2	
Outer shell body	Width	246	Stainless steel
	Height	209.5	
	Length	1670	
	Roof Radius	400	
	Thickness	0.8	
Outer shell floor plate	Width	246	Stainless steel
	Length	1670	
	Thickness	0.8	

## 3 Piezo-electric Patch Configuration (PPC)

A Piezo-electric Transducer (PZT) has electrical properties similar to that of a capacitor. It has two terminals. The PZT absorbs the strain energy in the objective structure caused due to bending deformations. The absorbed energy causes a charge distribution inside the PZT leading to potential

difference across its terminals. This phenomenon is called the Direct Piezo-electric effect. If a shunt circuit is connected across the PZT terminals, the current may be dissipated across the resistive elements of the shunt circuit in the form of joule heating resulting in suppression of vibrational deformation.

In order to damp multiple modes in the model, a single piezo-electric element (PZT) would not be enough. An array of piezo-electric elements, electrically connected in parallel configuration, localized around the point where we intend to suppress vibrational deformation, is termed as a Piezo-electric Patch Configuration (PPC). In this study, the number of PZT in a PPC is defined by the variable 'n' and the thickness of each PZT is defined by variable 't'. The standard PPC in this study consists of 10 C-6 PZT of Fuji ceramics corporations symmetrically localized around the floor plate center of the car-body, as shown in "Fig. 3". The physical and material specification the PZT utilized in this study is tabulated in "Table 3".

**Table 3. Specifications of PZT**

Property	notation	unit	value
Length	l	mm	80
Width	w	mm	25
Thickness	t	mm	0.3
Coupling factor	$k_{31}$	-	0.39
Dielectric constant	$\epsilon_{31}^T / \epsilon_0$	-	2270
Piezoelectric charge constant	$d_{31}$	C/N	$-210 \times 10^{-12}$
Poissons ratio	$\sigma$	-	0.32
Density	$\rho$	Kg/m <sup>3</sup>	7650

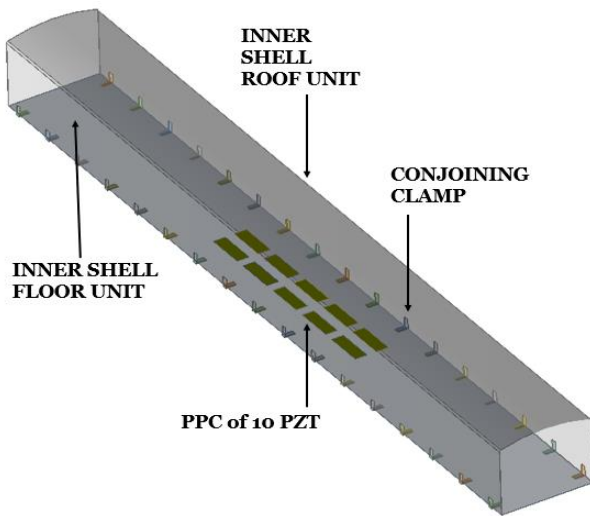


**Fig. 3. Piezo-electric patch configuration of 10 PZT elements (n = 10)**

## 4 Multi-mode Shunt circuit

In order to suppress bending vibrations on the floor of railway car-body, the proposed PPC is shunted by an electrical impedance. This technique is known as a semi-active shunt damping employing a shunt circuit. The simplest type of shunt circuit is the series L-R shunt circuit capable of damping a single bending mode only. Since, the objective is to damp multiple bending modes i.e. 3 modes , a multi-mode shunt circuit is utilized. The principle of this circuit is to parallelly connect three branches, each branch consisting of a current blocking circuit i.e. a parallel L-C circuit, in series with a L- R shunt circuit. Such type of shunt circuit, as in "Fig. 4" was proposed by Hollkamp [8].

This shunt circuit uses a lot of inductive elements which is difficult to emulate experimentally and also causes a lot of internal resistance in the circuit. A modified multi -mode shunt circuit [9], with lesser inductances, as in "Fig. 5", was utilized for this study.

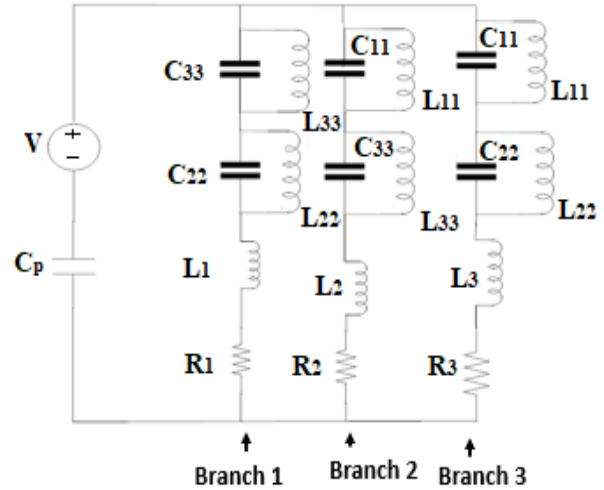


**Fig. 4. Multi-mode shunt circuit**

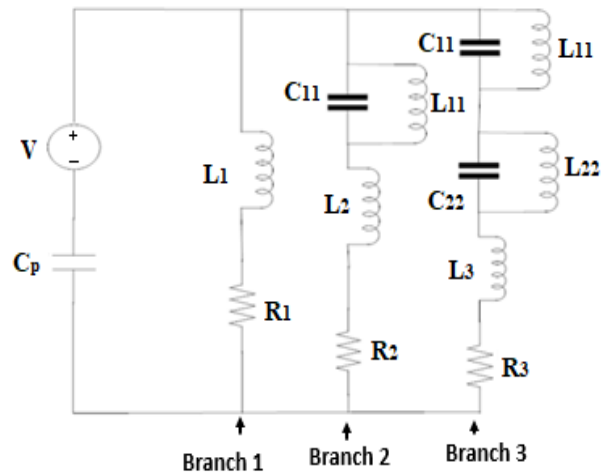


**Fig. 5. Modified Multi-mode shunt circuit**

## 5 Finite Element Modelling in ANSYS

Both the car-body models were modelled in ANSYS Workbench Design Modular. Solid 186 element was used to define the car-body shell. Body size meshing operation was done for the floor plate unit roof unit and clamps with element size of 2 cm for roof and floor. Conjoining and intermediate clamps had element size of 5 mm. Modal analysis and harmonic analysis were simulated to realize and compare the dynamic properties of both the car-body models. Coupled field analysis was further done to simulate the shunt circuit attached to the PPC and car-body.

### 5.1 Modal Analysis

Modal analysis in ANSYS workbench is an important tool to view the various mode shapes and natural frequencies of the objective structure in a set frequency range. The boundary conditions were simply supported. For the single shell model, first five bending modes were observed at frequencies of 58.36 Hz (shown in Fig. 6), 60.993 Hz, 69.29 Hz, 78.703 Hz and 84.863 Hz. The red zone in Fig. 6 indicates area of maximum strain energy. For the double shell model, these modes were observed at 43.36 Hz, 44.73 Hz, 66.47 Hz, 76.16 Hz and 85.63 Hz (shown in Fig. 7).

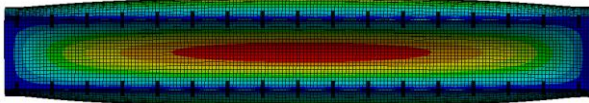


Fig. 6: First Bending mode shape of Single shell model observed on floor plate at 58.36 Hz

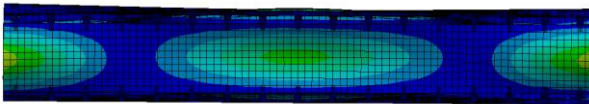


Fig. 7: Fifth Bending mode shape of Double shell model observed on floor plate at 85.63 Hz

### 5.2 Harmonic analysis

Harmonic analysis provides frequency response of the car-body models indicating the amplitude of car-body acceleration and displacement. A unit nodal force was applied at 332 mm distance from one end of the car-body inner shell floor. In double shell model the force was applied at the same point on the outer shell floor plate. Response was measured at the center of the inner shell floor in both the cases. Simply supported boundary condition was used. Self-damping coefficient of the railway car-body was assumed to be  $8 \times 10^{-3}$ . A bode plot of acceleration v/s frequency in the range 0-100 Hz showed car-body acceleration for single shell car-body have higher amplitudes than that

of double shell, shown in "Fig. 8".

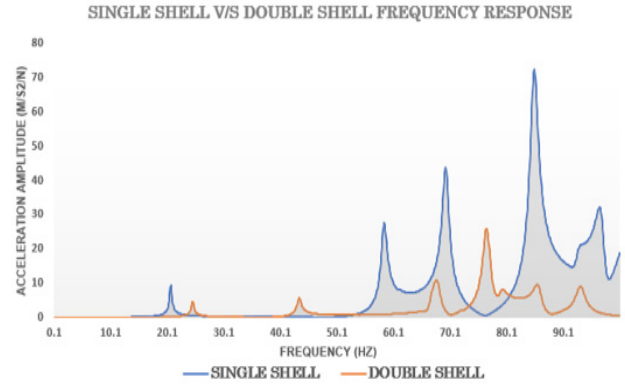


Fig. 8: Comparison of Single shell v/s Double shell frequency response

The comparison of undamped frequency responses of both the models clearly shows that the Double shell model has better dynamic characteristics since it has peak amplitudes of lesser magnitude than that of the single shell model. This is due to the intermediate clamping mechanism between the two shells which acts as a hanging connection as well as a vibration isolator. Based on the above observation, double shell model was considered for further simulation analysis, coupled field analysis and experimental analysis.

### 5.3 Coupled Field analysis

The finite element analysis in this study requires a structural electrical coupled field analysis. The PZT is defined using SOLID 226 elements having an additional voltage degree of freedom. CONTA174 and TARGE170 elements define the bonding between the PZT and the objective structure. CIRCU 94 elements define the inductance, resistance and capacitance used in the shunt circuit.

The governing equations for piezo-electric coupled field analysis [10] can be formulated as below

$$\begin{bmatrix} M_{UU} & 0 \\ 0 & 0 \end{bmatrix} \begin{Bmatrix} \ddot{U} \\ \ddot{V} \end{Bmatrix} + \begin{bmatrix} C_{UU} & 0 \\ 0 & -C_{VV} \end{bmatrix} \begin{Bmatrix} \dot{U} \\ \dot{V} \end{Bmatrix} + \begin{bmatrix} K_{UU} & K_{UV} \\ K_{UV}^T & -K_{VV} \end{bmatrix} \begin{Bmatrix} U \\ V \end{Bmatrix} = \begin{Bmatrix} F \\ Q \end{Bmatrix} \quad (1)$$

Where, U is the nodal displacement force, V is the nodal voltage,  $K_{UU}$  is the structural stiffness matrix,  $K_{VV}$  is the dielectric permittivity matrix,  $K_{UV}$  is the piezo-electric coupling matrix,  $C_{UU}$  is the structural damping matrix,  $C_{UV}$  is the dielectric dissipation matrix,  $M_{UU}$  is the mass matrix and F is the element force.

The values of the shunt circuit elements such as the inductive, resistive and capacitive elements in the circuit shown in Fig. 5 can be obtained by formulations used by Hagood et al [11] and Shu-yau [9].

$$L' = 1 / [\omega_n^2 C_p (1 + K_i^2)] \quad - (2)$$

$$R' = 2^{1/2} K_i / [\omega_n C_p (1 + K_i^2)] \quad - (3)$$

$$K_i^2 = (\omega_{no}^2 - \omega_{ns}^2) / \omega_{ns}^2 \quad - (4)$$

$$L_{11} C_{11} = 1 / \omega_1^2 \quad - (5)$$

$$L_{22} C_{22} = 1 / \omega_2^2 \quad - (6)$$

$$L_2 = \frac{L_1' L_2' + L_2' L_{11} - L_1' L_{11} - (\omega_2^2 / \omega_1^2) L_1' L_2'}{(L_1' - L_2') (1 - \omega_2^2 / \omega_1^2)} \quad - (7)$$

$$L_3 = A - B \quad - (8)$$

$$A = \frac{L_1' L_3' [L_{11} + L_2 - (\omega_3^2 / \omega_1^2) L_2]}{(L_1' - L_3') (L_{11} + L_2 - (\omega_3^2 / \omega_1^2) L_2) - L_1' L_3' (1 - \omega_3^2 / \omega_1^2)} \quad - (9)$$

$$B = \frac{L_{11} + L_{22} - (\omega_3^2 / \omega_2^2) L_{11} - (\omega_3^2 / \omega_1^2) L_2}{(1 - \omega_3^2 / \omega_2^2) (1 - \omega_3^2 / \omega_1^2)} \quad - (10)$$

$$R_2 = \frac{R_1' R_2'}{(R_1' - R_2')} \quad - (11)$$

$$R_3 = \frac{R_1' R_2' R_3'}{(R_1' R_2 - R_2' R_3 - R_1' R_3')} \quad - (12)$$

where,  $L'$  is the optimum inductance for single mode damping,  $\omega_n$  is the modal frequency,  $C_p$  is the piezo-electric capacitance,  $K_i$  is the generalized electro-mechanical coupling coefficient for 'i'<sup>th</sup> mode  $R'$  is the optimum resistance for single mode damping,  $\omega_{no}$  is the modal frequency of car-body with bonded PPC in open circuit condition,  $\omega_{ns}$  is modal frequency with bonded PPC in shorted condition,  $\omega_1$ ,  $\omega_2$  and  $\omega_3$  are the three target bending mode frequencies respectively, such that  $\omega_1 < \omega_2 < \omega_3$ ,  $L_{11}$  and  $C_{11}$  are the parameters for branch 1 anti-resonant circuit,  $L_{22}$  and  $C_{22}$  are the parameters for branch 2 anti-resonant circuit.  $L_2$  and  $L_3$  are optimum inductance for branch 2 and branch 3 of shunt circuit respectively.  $R_2$  and  $R_3$  are optimum resistance for branch 2 and branch 3 of shunt circuit.

Mode numbers 1,4 and 5 of the double shell model were chosen as target modes for multi-modal damping. Using the above formulations for the PPC configuration of  $n=10, t=0.3$  mm, the shunt circuit parameters to damp the target modes, in simulation analysis, was obtained as  $L_1 = L_1' = 15$  H,  $L_2 = 39.5$  H,  $L_3 = 342.25$ ,  $R_1 = 170$   $\Omega$ ,  $R_2 = 180$   $\Omega$ ,  $R_3 = 365$   $\Omega$ ,  $L_{11} = 67.2$  H,  $L_{22} = 21.9$ ,  $C_{11} = C_{22} = 200$  nF.

The multi-mode damping in simulation analysis was realized by inputting these parametric values as APDL commands in the ANSYS harmonic window.

```
/prep7
n,node,1,1,0
n,node,1,0.9,0
n,node,1,0.8,0
n,node,1,0.7,0
n,node,1,0.6,0
n,node,1,0.5,0
allsel
cmsel,s,PZT_BOT
cp,1,volt,all
*get,nbot,node,0,num,min
```

```
cmsel,u,PZT_BOT
cmsel,s,PZT_TOP
cp,2,volt,all
*get,ntop,node,0,num,min
cmsel,u,PZT_TOP
allsel
et,817,circu94,1
r,817,15
type,817$real,817
e,69249,ntop
et,818,circu94,0
r,818,170
type,818$real,818
e,69249,nbot
et,819,circu94,1
r,819,67.24
type,819$real,819
e,69250,ntop
et,820,circu94,2
r,820,200e-09
type,820$real,820
e,69250,ntop
et,821,circu94,1
r,821,39.5
type,821$real,821
e,69250,69251
et,822,circu94,0
r,822,180
type,822$real,822
e,69251,nbot
et,823,circu94,1
r,823,67.24
type,823$real,823
e,69252,ntop
et,824,circu94,2
r,824,200e-09
type,824$real,824
e,69252,ntop
et,825,circu94,1
r,825,21.9
type,825$real,825
e,69252,69253
et,826,circu94,2
r,826,200e-09
type,826$real,826
e,69252,69253
et,827,circu94,1
r,827,342.25
type,827$real,827
e,69253,69254
et,828,circu94,0
r,828,365
type,828$real,828
e,69254,nbot
allsel
finish
/solve
```

## 6 Experimental analysis

The experimental set up consists of a 1/12<sup>th</sup> scaled double shell car-body model simply supported on both the ends. The harmonic excitation is applied at 332 mm from one end of the car-body on the outer shell floor. This point is chosen to avoid applying any force at a nodal point of any of the natural frequencies of the objective structure in the range of 0-100 Hz. The sinusoidal harmonic input in the range of 0-100 Hz was

provided by an electro-dynamic shaker (K2004E004) connected to a force transducer (PCB 20B-C03). The WE7000 YOKOGAWA function generator provides the input to the shaker. The response from the car-body is measured the centre of the inner shell floor plate by a piezotronics accelerometer. The response data is processed in the ONO SOKKI DS-2104 FFT analyser. The schematic of experimental set-up is shown in Fig.8.

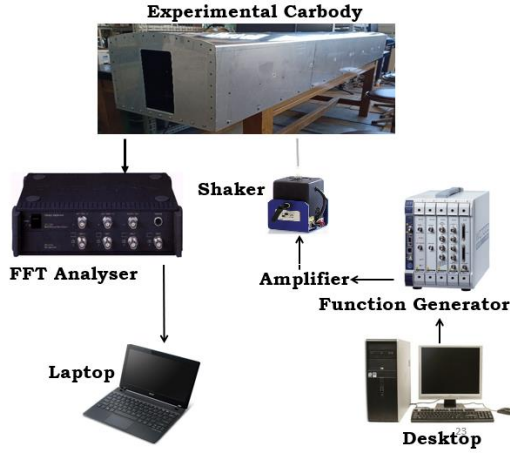


Fig. 8: Schematic of the experimental set up

The experimental frequency response of double shell car-body model (without PPC) showed peaks at frequencies of 56 Hz, 79.5 Hz, 84 Hz and 92.75 Hz, described in Fig. 9, which are the first, third, fourth and fifth bending mode. The shunt circuit was designed in order to damp the first, fourth and fifth bending modes, since these modes were observable as well as controllable.

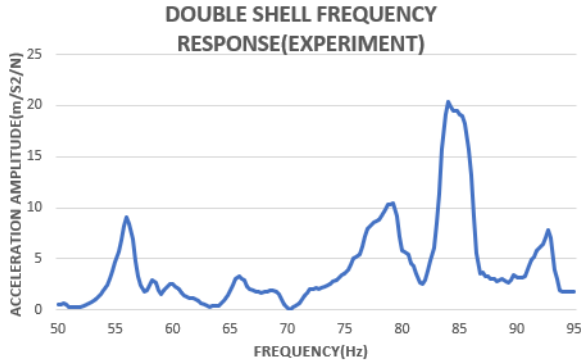


Fig. 9: Experimental frequency response of double shell model

The PPC consisting of 10 C-6 PZT elements was physically bonded to the inner shell floor plate with epoxy resin. Using the equations 2-12 we obtain the shunt circuit parameters for experimental model as  $L_1 = 8.5$  H,  $L_2 = 20.18$  H,  $L_3 = 138.68$  H,  $R_1 = 70$   $\Omega$ ,  $R_2 = 126$   $\Omega$ ,  $R_3 = 360$   $\Omega$ ,  $L_{11} = 17.03$  H,  $L_{22} = 11.25$  H,  $C_{11} = 474$  nF,  $C_{22} = 319$  nF. Since the inductance values are on the higher side, Gyrator circuits were used to virtually realize inductances, as shown in Fig. 10. These gyrator circuits are made using combination of

LF-356N operational amplifiers, resistors and capacitors. Op-amps require constant voltage power input of  $\pm 12$  V, thus making it a semi-active shunt circuit.

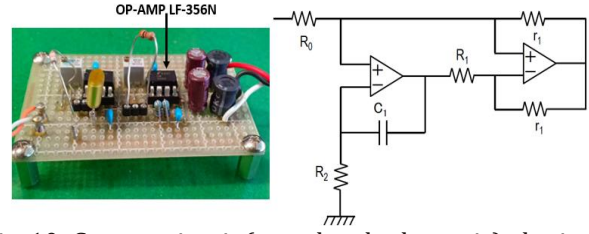


Fig. 10: Gyrator circuit (actual and schematic) obtained from RTRI

## 7 Simulation Results

### 7.1 PPC consisting of $n = 10$ , $t = 0.3$ mm

The simulation results of the double shell model in damped and undamped condition for  $n=10$ ,  $t= 0.3$  mm PPC, were compared individually for the first, fourth and fifth bending mode in Fig. 11,12 & 13 respectively.

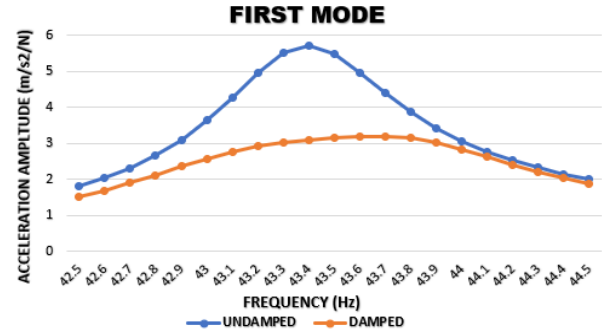


Fig.11: Simulation frequency response Mode-1

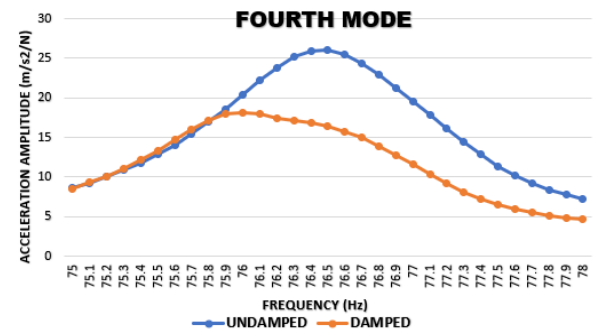


Fig.12: Simulation frequency response Mode-4

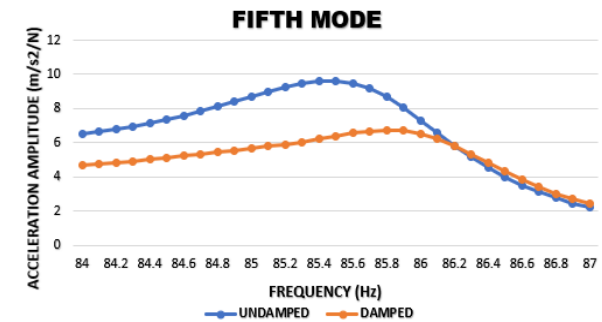


Fig. 13: Simulation frequency response Mode-5

For the  $n=10$ ,  $t=0.3$  mm configuration, the tuned multi-mode shunt circuit induced vibration suppression of 44%, 30% and 29% for the first, fourth and fifth bending modes.

## 7.2 PPC consisting of $n = 10$ and $t = 0.3, 0.5, 0.8, 1.0$ mm

In order to determine the effect of varying the PZT thickness on damping performance of PPC, PZT thickness of 0.3mm, 0.5 mm, 0.8 mm and 1 mm were simulated. The damping performance for modes 1,4 and 5 are shown below in Fig .14,15 and 16.

It was observed that for Mode-1,  $t=0.8$  mm showed the best damping performance. Similarly, for Mode-4 and Mode-5,  $t = 0.8$  mm and  $t = 1$  mm respectively, showed the best vibration suppression performance.

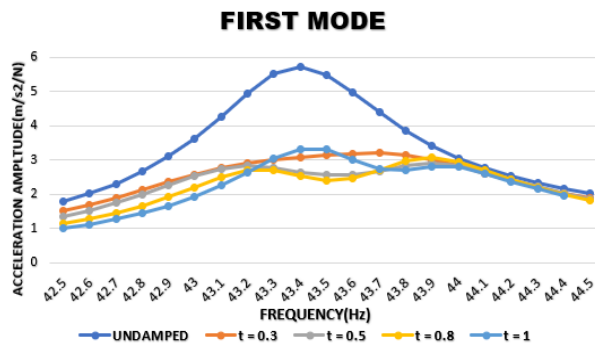


Fig. 14: Mode-1 response for varying PZT thickness

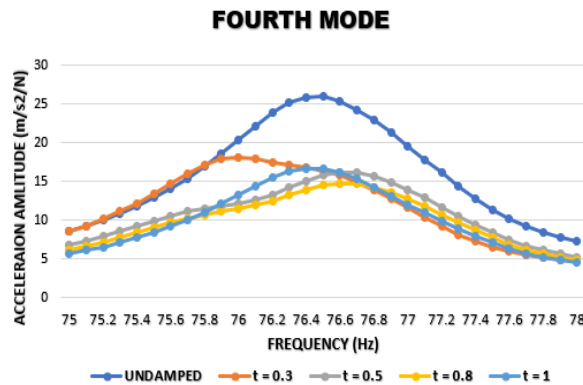


Fig. 15 :Mode-4 response for varying PZT thickness

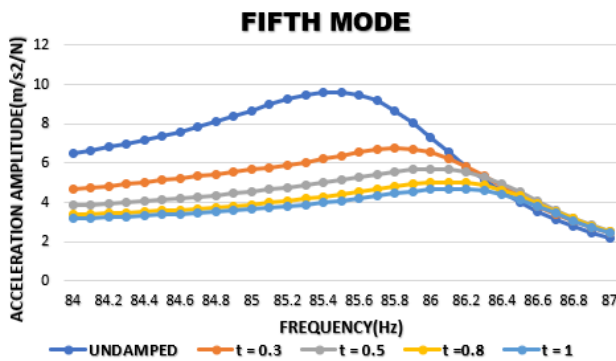


Fig. 16: Mode-5 response for varying PZT thickness

## 7.3 PPC of $n = 10, 14$ and $18$ and $t = 0.3$ mm

The impact of PPC configurations with higher number of PZT was further studied by simulating PPCs of 10,14 and 18 piezoelectric elements. It was observed that for mode-1,  $n=10$  PPC showed the best vibration suppression results, as in Fig 17. For mode-4,5 vibration suppression results of  $n=10$  and  $n=14$  were roughly identical. PPC of  $n=18$  showed the worst vibration suppression performance. This shows that a PPC, confined to the region of maximum strain energy in the car-body, will provide better vibration suppression.

## 8 Experimental Results

The experimental results of double shell car-body model with  $n=10$ ,  $t=0.3$  mm PPC is shown below in “Fig. 18, 19 and 20”. Experimental analysis results with the 1/12<sup>th</sup> scale double shell car-body model with bonded PPC connected to a tuned multi-mode circuit showed vibration amplitude reduction of 49%, 21% and 19% for first, fourth and fifth bending modes respectively. In decibel terms, 5.85 dB, 2.05 dB and 1.83 dB damping were attained for the target modes.

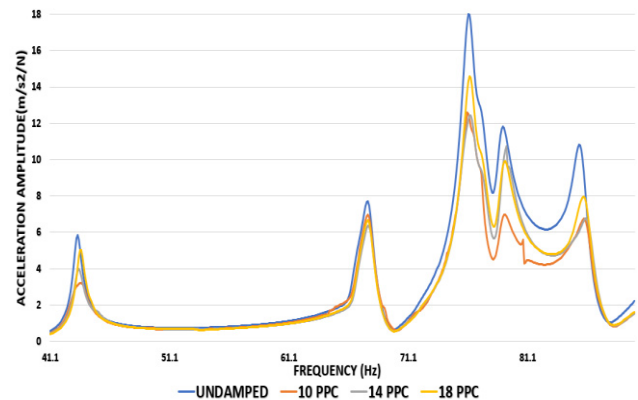


Fig. 17: Double shell response for different PPC

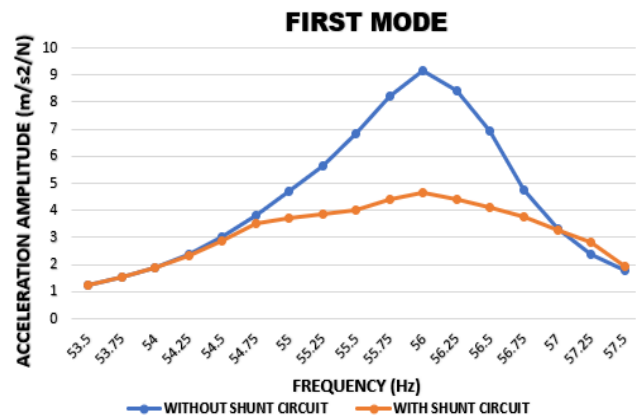


Fig. 18: Experimental frequency response Mode-1

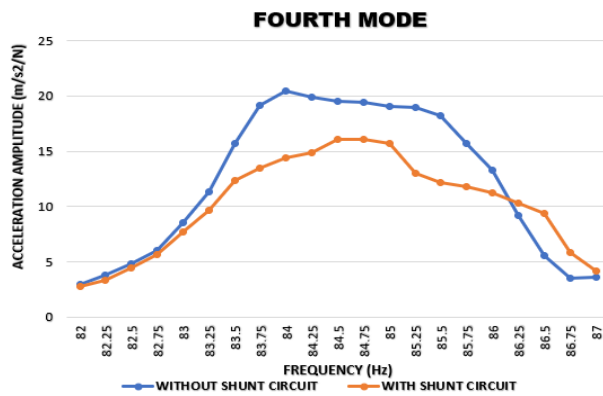


Fig. 19: Experimental frequency response Mode-4

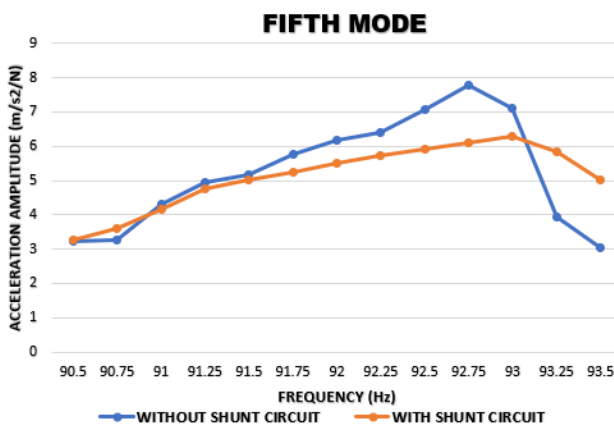


Fig. 20: Experimental frequency response Mode-5

## 9 Conclusion

In this paper, vibration characteristics of a railway car-body model was studied by comparing the single shell model with the double shell model. It was observed that the double shell model had better dynamic characteristics and hence better ride quality for passengers. Further study was done to analyse the impact of an integrated semi-active multi-mode shunt circuit on the vibration characteristics of the double shell model. In case of an  $n=10$ ,  $t=0.3$  mm PPC, Simulation analysis in ANSYS 17.1 showed vibration suppression of 5.03 dB, 3.10 dB and 2.97 dB for the targeted modes, whereas vibration suppression of 5.85 dB, 2.05 dB and 1.83 dB for the target modes was attained in the experimental set-up. A satisfactory co-relation was observed between the simulation and experimental results. The impact of increasing the PZT thickness on the damping performance was studied and it was inferred that better vibration damping is achieved when the thickness of the PZT is equal to the thickness of floor plate, i.e.  $t=0.8$  mm. Increasing the number of PZT elements in the PPC did not show any direct relation to improvement in damping performance. Overall  $n=10$  configuration of PPC exhibited better damping performance. Differences in modal frequencies, acceleration amplitudes and damping between the

simulation and experimental model can be attributed to car-body modelling error, PZT hysteresis loss, breadboard losses and non-linearity. Although the semi-active control technique is not robust, but it is cost effective and does not have any stability issues.

## References

- [1] A. Orvnas : Method for reducing vertical car-body vibration of a rail vehicle, *Report in Railway Technology Stockholm, Sweden 2010*
- [2] Railway applications- Ride comfort for passengers - Measurement and evaluation, *CEN, EN 12299 Brussels April 2009*
- [3] A. E. J. Hardy, and R. R. K. Jones, Control of the noise environment for passengers in railway vehicles, *Proc. Inst. Mech. Eng.,203F*, pp. 79–85, 1989.
- [4] P. Carlbom: Structural flexibility in a rail vehicle car body, *KTH/FKT/FR 98/37*, Division of Railway Technology, Department of Vehicle Engineering, KTH (1998)
- [5] T. Takigami, and T. Tomioka,: Investigation to suppress bending vibration of railway vehicle car-bodies using piezoelectric elements. *Q. Rep. RTRI*, 2005, **46**(4), pp. 225–230.
- [6] K. Ishiguri, Y. Kobayashi, T. Tomioka and Y. Hoshino, Vibration Analysis of a Railway Car-body Using a Shell Model, *Journal of System Design and Dynamics Vol 2*,2006.
- [7] A. Gautam, Y. Kobayashi, T. Emaru and K. Yamamoto, "Vibro-Acoustic Analysis of Double shell structure for Railway Carbody Model" –*The 17<sup>th</sup> Asia Pacific Vibration Conference, Nanjing, China*.
- [8] Joseph J. Hollkamp- "Multimodal Passive Vibration Suppression with Piezoelectric Materials and Resonant Shunts",*Journal of Intelligent Material Systems and Structures 1994 5*: 49.
- [9] Shu-yau Wu ,“Method for multiple mode shunt damping of structural vibration using a single PZT transducer” – *Journal of Intelligent Material System and Structures*, Volume: 9 issue: 12, page(s): 991-998.
- [10] ANSYS Mechanical APDL and Mechanical Applications Element Reference, 2013.
- [11] N. W. Hagood and A. Von Flotow, “Damping of Structural Vibrations with Piezoelectric Materials and Passive Electrical Networks” - *Journal of Sound and Vibration* (1991) **146**(2), pp. 243-268